

Article

The Generation of Circularly Polarized Isolated Attosecond Pulses with Tunable Helicity from CO Molecules in Polarization Gating Laser Fields

Shiju Chen ¹, Hua Yuan ^{1,*}, Feng Wang ^{2,*}, Jiahang Song ¹, Yue Zhao ¹, Chunhui Yang ², Tianxin Ou ², Ru Zhang ², Qiang Chang ¹ and Yuping Sun ¹

¹ School of Physics and Optoelectronic Engineering, Shandong University of Technology, Zibo 255049, China; changqiang@sdut.edu.cn (Q.C.); sunyuping@sdut.edu.cn (Y.S.)

² Hubei Key Laboratory of Optical Information and Pattern Recognition, Wuhan Institute of Technology, Wuhan 430205, China

* Correspondence: yuanhua@sdut.edu.cn (H.Y.); wangfeng@wit.edu.cn (F.W.)

Abstract: We theoretically demonstrate a scheme to generate circularly polarized (CP) isolated attosecond pulses (IAPs) with tunable helicity using a polarization gating laser field interacting with the CO molecule. The results show that a broadband CP supercontinuum is produced from the oriented CO molecule, which supports the generation of an IAP with an ellipticity of 0.98 and a duration of 90 as. Furthermore, the helicity of the generated harmonics and IAP can be effectively controlled by modulating the laser field and the orientation angle of the CO molecule. Our method will advance research on chiral-specific dynamics and magnetic circular dichroism on the attosecond timescale.

Keywords: circularly polarized isolated attosecond pulse; high-order harmonic generation; polarization gating laser field; tunable helicity



Citation: Chen, S.; Yuan, H.; Wang, F.; Song, J.; Zhao, Y.; Yang, C.; Ou, T.; Zhang, R.; Chang, Q.; Sun, Y. The Generation of Circularly Polarized Isolated Attosecond Pulses with Tunable Helicity from CO Molecules in Polarization Gating Laser Fields. *Photonics* **2024**, *11*, 464. <https://doi.org/10.3390/photonics11050464>

Received: 12 March 2024

Revised: 28 April 2024

Accepted: 29 April 2024

Published: 15 May 2024



Copyright: © 2024 by the authors. Licensee MDPI, Basel, Switzerland. This article is an open access article distributed under the terms and conditions of the Creative Commons Attribution (CC BY) license (<https://creativecommons.org/licenses/by/4.0/>).

1. Introduction

High-order harmonic generation (HHG) is an extremely nonlinear optical process that results from the interaction of an intense laser with atoms, molecules, and solids [1,2]. It can be well understood by the semiclassical three-step model [3]. Firstly, the electrons are ionized from the ground state and elevated to the continuum through tunneling ionization. Subsequently, the ionized electrons, which can be considered as free electrons, accelerate in the laser field. In the final step, some of these electrons can recombine with the parent ion, and the high-order harmonics are released from the transition to the ground state, which can reach the extreme ultraviolet (EUV) or soft X-ray region [4,5]. The HHG process repeats every half laser optical cycle, resulting in the generation of attosecond pulses in a train. Since isolated attosecond pulses (IAPs) are preferred in some special applications that involve measuring electron ionization and other ultrafast processes in matter [6,7], many efforts have been dedicated to generating IAP sources, making great progress in recent years. Numerous approaches have been proposed for generating an IAP, such as utilizing few-cycle laser pulses [8,9], employing two-color or multi-color fields [10–14], and using the polarization gating (PG) technique [15–20]. However, most of these methods focus on generating a linearly polarized (LP) IAP. Recently, circularly polarized (CP) or largely elliptically polarized (EP) attosecond pulses have gained considerable attention due to their applications in detecting circular dichroism in magnetic materials and chiral recognition [21–25]. Consequently, many efforts have been devoted to generating these pulses [25–38].

So far, two categories of schemes have been proposed for generating CP or largely EP attosecond pulses. The first is using specific laser fields to control the HHG process. It has

been demonstrated that the CP harmonics can be generated by employing a bichromatic counter-rotating CP laser field [29–33]. However, this method produces two adjacent harmonics with alternating helicities (left and right helicities), which hinder the generation of CP attosecond pulses. Additionally, the utilization of a pair of counter-rotating CP pulses in a noncollinear geometry has been proven effective in generating pure CP harmonics [34]. The generated harmonics with left and right helicities can be spatially separated, facilitating the production of pure CP attosecond pulses with a specific helicity. Recently, a new approach has been proposed for generating EP attosecond pulses by employing two-color cross-LP laser fields [35].

Another category of schemes to generate CP or largely EP attosecond pulses focusses on HHG from molecule targets. The transition dipole moment for HHG relies on the electronic structure of targets. Compared to atoms with an isotropic structure, the molecules possess more complex structures and symmetries, which therefore influence the transition dipole moment as well as HHG. By directly interacting ana LP laser field with aligned symmetric molecules (N₂, O₂, or CO₂), EP harmonics can be generated [36,37]. However, these harmonics are confined to a few harmonic orders and possess small ellipticity. Another method proposes to use the Ar–N₂ mixed medium as the target to obtain the EP attosecond pulse [38].

In this paper, we propose the production of CP IAPs by employing the PG laser field. This laser field, composed of two counter-rotating CP laser pulses with a time delay, has been widely used both theoretically and experimentally for generating LP high-order harmonics and IAPs; now, it is extended to produce CP high-order harmonics and IAPs with the CO molecule. The results show that a sub-100 as IAP with an ellipticity of 0.98 can be obtained from the oriented CO molecule. Moreover, the generation of the CP IAP is robust against the variation in the time delay of two CP pulses. Moreover, effective control over the helicity of the generated IAP can be achieved by adjusting the laser field and the molecular orientation.

2. Theoretical Model

In our simulations, we consider high photon energies so that we can neglect the Coulomb effect of these harmonics [39,40]. Therefore, the extended Lewenstein model is used in our simulations [41]. The x, y components of the time-dependent dipole moment can be written as (in atomic units):

$$D_j(t, \theta) = i \int_{-\infty}^t dt' \left[\frac{\pi}{\xi + i(t-t')/2} \right]^{3/2} E(t') g(t', \theta) \times d_j^* [p_{st}(t', t) - A(t), \theta] e^{-iS_{st}(t', t)} \times d_j [p_{st}(t', t) - A(t'), \theta] + c.c., \quad j = x, y, \quad (1)$$

where ξ is a positive regularization constant and $g(t', \theta) = e^{[-\int_{-\infty}^{t'} w(t', \theta) dt']}$ is the ground state amplitude with the ionization rate $w(t', \theta)$, calculated by the molecular Ammosov–Delone–Krainov (MO-ADK) model [42]. d_j represents the dipole matrix element from the ground state to the continuum, characterized by the electron velocity v ($v = p_{st} - A$), which is expressed as

$$d(v, \theta) = \langle \psi_0(R, \theta) | R | v \rangle, \quad (2)$$

where $\psi_0(R, \theta)$ is the ground state of the CO molecule, which is obtained through an ab initio calculation using a 6-31 G * basis set in the Gaussian software package. p_{st} and S_{st} are the stationary momentum and quasiclassical action, respectively, and are given by

$$p_{st}(t', t) = \frac{1}{t - t'} \int_{t'}^t A(t'') dt'' \quad (3)$$

$$S_{st}(t', t) = \int_{t'}^t dt'' \left\{ \frac{1}{2} [p_{st}(t', t) - A(t'')]^2 + I_p \right\}. \quad (4)$$

Here, I_p is the ionization potential of the CO molecule, which is 14 eV. $A(t)$ is the vector potential of the driving electric field, $E(t)$. In our simulations, we used the PG laser field, of which the x, y components are given by

$$E_x(t) = E_0 \left\{ e^{-2\ln(2)[(t-T_d/2)/\tau_p]^2} + e^{-2\ln(2)[(t+T_d/2)/\tau_p]^2} \right\} \times \cos(\omega t + \varphi_{CE}) \quad (5)$$

$$E_y(t) = E_0 \left\{ e^{-2\ln(2)[(t-T_d/2)/\tau_p]^2} - e^{-2\ln(2)[(t+T_d/2)/\tau_p]^2} \right\} \times \sin(\omega t + \varphi_{CE}), \quad (6)$$

where E_0 and ω are the amplitude and frequency of these two CP laser pulses, whose intensity is $3 \times 10^{14} \text{W/cm}^2$ and wavelength is 1600 nm. A laser field with such an intense intensity and a long wavelength was chosen in order to minimize the influence of the Coulomb effect on the continuum electron during the HHG process. The carrier-envelope phase (CEP) is represented by φ_{CE} , which was set to 0.8π . τ_p corresponds to the pulse duration of the laser field, which was $2T_0$, with the optical cycle, T_0 , of the laser field. T_d is the time delay between two CP laser pulses, which was chosen to be $1.8T_0$. The CO molecule was assumed to be oriented in the x–y plane. θ is the orientation angle between the positive x-axis and the molecular axis. A value of θ at 0° indicates that the O center lies on the positive x-axis.

The harmonic spectrum is obtained by Fourier transforming the time-dependent dipole acceleration, which is expressed as

$$a_j(q, \theta) = \frac{1}{T} \int_0^T \ddot{D}_j(t, \theta) e^{-iq\omega t} dt. \quad (7)$$

Here, T is the duration of the laser field and q represents the harmonic order. The time-step size, dt , is 0.1, which is sufficient to reach convergence (i.e., no observable change in the results by further increasing and decreasing). The intensity and phase of the harmonics are obtained by $I_j = |a_j(q, \theta)|^2$ and $\varphi_j(q, \theta) = \text{arg}[a_j(q, \theta)]$, respectively. The relative phase of the x and y harmonic components is defined as $\delta = \varphi_y - \varphi_x$. When δ equals 0 or $-\pi$, the harmonic will be LP. Otherwise, it will be EP or CP. The intensity of the left CP (LCP) and right CP (RCP) harmonic components can be obtained by

$$I_{\pm} = |a_{\pm}|^2, \quad (8)$$

where $a_{\pm}(q, \theta) = \frac{1}{\sqrt{2}} [a_x(q, \theta) \pm ia_y(q, \theta)]$.

3. Results and Discussion

Firstly, we investigated the generation of a CP IAP from the CO molecule by the PG laser field. The electric field of the PG is depicted in Figure 1a. We can see that the laser field is EP at the leading and trailing edges of the laser pulse and becomes linear polarization at the pulse center, referred to as the gate of PG. The gate width, δt , is $0.32T_0$, which is calculated by $\delta t_{\varepsilon=0.1} = \frac{1}{\ln 2} \varepsilon \frac{\tau_p^2}{T_d}$. The generated harmonic spectrum from the CO molecule oriented at $\theta = 280^\circ$ is shown in Figure 1b. It can be observed that the x and y components of the harmonic spectrum have the same cutoff, at about the 690th-order harmonic. Additionally, these two harmonic components both exit a supercontinuum ranging from the 300th to 690th orders, displaying comparable intensities. We further calculated the relative phase between the x and y harmonic components, as inserted in Figure 1b. The relative phase between the x and y components of these harmonics is close to 0.5π . This finding is attributed to the asymmetry of the molecular orbital of CO. The relative phase of 0.5π , along with the approximately identical intensities of the x and y harmonic components, indicates that the generated harmonics in the supercontinuum region may be CP. For a further insight into the polarization characteristics of the generated harmonics, we present the LCP and RCP components of the harmonic spectrum in Figure 1c. One can see that the intensity of the LCP harmonic components surpasses that of the RCP component, particularly in the range from the 300th to 600th orders, where it is approximately 1.5 orders

of magnitude higher than that of the RCP component. This means that the harmonics in the supercontinuum region have left helicity. In Figure 1d,e, we present the time–frequency distributions for the x and y components of the harmonics to gain a better understanding of the generation of the supercontinuum. Both the x and y harmonic components exhibit one dominant emission peak (marked by P_1) at around $5.3T_0$ for the harmonics above the 300th order. This behavior arises from the strong dependence of HHG efficiency on the time-dependent ellipticity of the PG laser field. Moreover, within this emission peak, the intensity of the short quantum path is significantly higher than that of the long path. Therefore, a broadband supercontinuum was obtained (see Figure 1b), which can support the generation of an IAP. By superposing the 360th- to 440th-order harmonics in the supercontinuum, we derived an IAP with left helicity, as shown in Figure 1f. We calculated the ellipticity of this IAP by determining the ratio of the minor axis to the major axis of the largest ellipse formed by the projection of the electric vector, which is 0.98, very close to circular polarization. The duration of this IAP is estimated to be approximately 90 as.

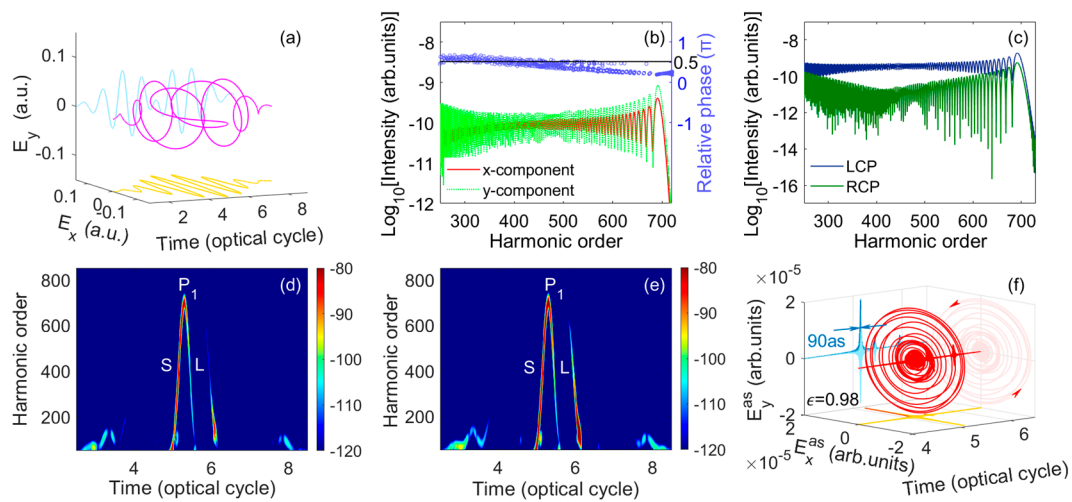


Figure 1. (a) The 3D plot of the PG laser field (purple line). The x, y components of the electric field (orange and blue lines). (b) The x, y components of the generated harmonic spectrum with the CO molecule oriented at $\theta = 280^\circ$. The corresponding relative phases of the x, y components are also inserted as the blue circles. A black solid line indicates the relative phase of 0.5π . (c) The LCP and RCP components of the generated harmonic spectrum. (d,e) The corresponding time–frequency distributions of the x and y components of the harmonics. (f) The 3D plot of the electric field of the attosecond pulse generated by superposing the 360th- to 440th-order harmonics in (b).

The time delay, T_d , between two counter-rotating CP laser pulses can influence the gate width, $\delta t_{\epsilon=0.1}$, of the PG, subsequently impacting the generated harmonic spectrum as well as IAP. We next present the generated harmonic spectrums and attosecond pulses for T_d of $1.6T_0$, $1.9T_0$, and $2.2T_0$ in Figure 2 to investigate its dependence on T_d . Figure 2a–c demonstrate that although T_d varies, we can still derive a supercontinuum within a broad region. Furthermore, within the supercontinuum region, the intensity of the LCP harmonic component surpasses that of the RCP component in all three cases. Through the superposition of harmonics (the 360th to 440th orders) in the supercontinuum, IAPs are obtained, as depicted in Figure 2d–f. It is obvious that the variation in T_d has a minor influence on the ellipticities of the IAPs, all of which exceed 0.87. However, the change in T_d significantly affects the IAPs, resulting in longer durations.

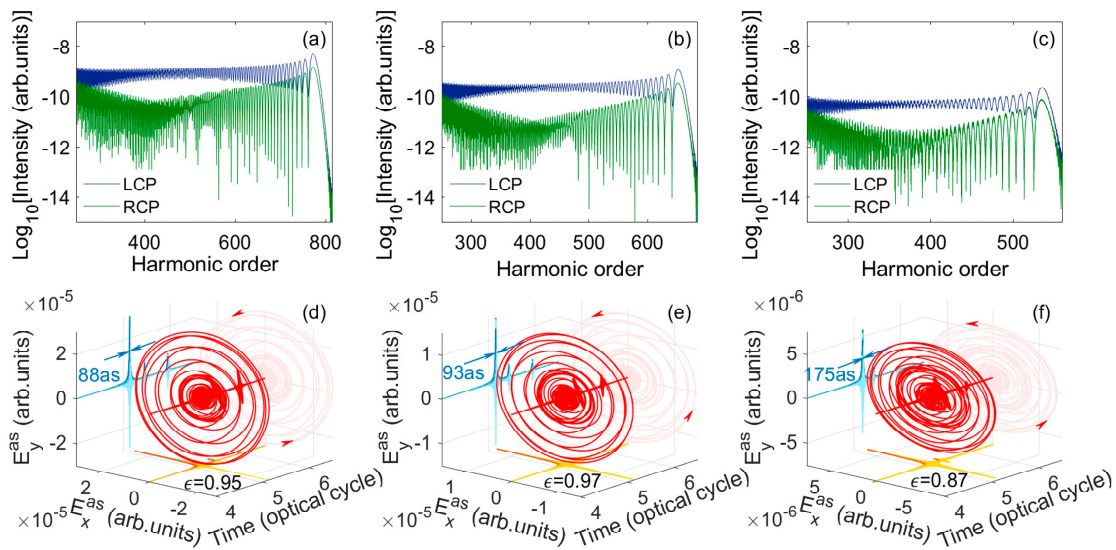


Figure 2. (a–c) The LCP and RCP components of the harmonic spectra generated from the CO molecule oriented at $\theta = 280^\circ$ in the PG laser field for the time delays, T_d , of the laser fields of $1.6T_0$, $1.9T_0$, and $2.2T_0$, respectively. (d–f) The 3D plots of the electric fields of the attosecond pulses generated by superposing the 360th- to 440th-order harmonics in (a–c), respectively. In our simulations, except for the time delay, T_d , other parameters are the same as those in Figure 1.

Here, we investigate the influence of the CEP, i.e., φ_{CE} , of the laser field on the generated harmonic spectrum and attosecond pulse. Figure 3a–c present the harmonic spectrums for φ_{CE} of -0.3π , 0.7π and 0.9π . The generated attosecond pulses are shown in Figure 3d–f. For $\varphi_{CE} = -0.3\pi$, it can be observed from Figure 3a that a broadband supercontinuum spanning from the 300th to 690th orders is generated. However, unlike the case of $\varphi_{CE} = 0.8\pi$ presented in Figure 1c, the intensity of the RCP component of harmonics in the supercontinuum here exceeds that of the LCP component. Especially for the harmonics from the 360th to 440th orders, the intensity of the RCP harmonic component is about one order of magnitude higher than that of the LCP component. By superposing these harmonics, an IAP with right helicity is generated with an ellipticity of 0.79 and a duration of 91 as, as shown in Figure 3d. As for $\varphi_{CE} = 0.7\pi$ in Figure 3b, we can still derive a supercontinuum in the region from the 300th to 690th orders. In this case, the intensity of the LCP harmonic component surpasses that of the RCP component. Then, superposing the 320th- to 360th-order harmonics, we derive a left-rotated IAP of which the ellipticity is 0.67 and the duration is 162 as, as shown in Figure 3e. In the case of $\varphi_{CE} = 0.9\pi$, a supercontinuum ranging from the 640th to 700th orders is generated (see Figure 3c). Moreover, the intensity difference between the LCP and RCP harmonic components becomes smaller in comparison to the case of $\varphi_{CE} = 0.7\pi$ in Figure 3b. Superposing the 640th- to 700th-order harmonics, we derive a left-rotated IAP whose ellipticity is only 0.39 and a duration of 192 as, as presented in Figure 3f.

Since the molecular orientation may influence the dipole matrix element, as presented in Equation (2), which, in turn, affects the HHG and attosecond pulse generation, we next investigate the effect of molecular orientation on the generated harmonic spectrum and attosecond pulse. Figures 4a–c and 4d–f are the generated harmonic spectrums and attosecond pulses from the CO molecule for orientation angles of 100° , 275° , and 285° , respectively. As we can see from Figure 4a, when the CO molecule is oriented at 100° , a supercontinuum spanning from the 300th to 690th orders is produced. Within this range, the intensity of the RCP harmonic component is approximately one order of magnitude higher than that of the LCP component. Superposing the 460th- to 540th-order harmonics yields a right EP IAP with an ellipticity of 0.69 and a duration of 93 as (see Figure 4d). When the orientation angle of the CO molecule is tuned to 275° (Figure 4b), the supercontinuum

ranging from the 300th to 690th orders can also be obtained, but the intensity of the LCP harmonic component is much higher than that of the RCP component. This, in turn, results in the generation of a left-rotated IAP with an ellipticity of 0.53 and a duration of 93 as by superposing the 480th- to 560th-order harmonics, as shown in Figure 4e. As the molecular orientation angle changes to 285° in Figure 4c, the intensities of the LCP and RCP harmonic components become comparable. When we superpose the 310th- to 390th-order harmonics, we derive an IAP with a small ellipticity of 0.33 and a duration of 102 as (see Figure 4f).

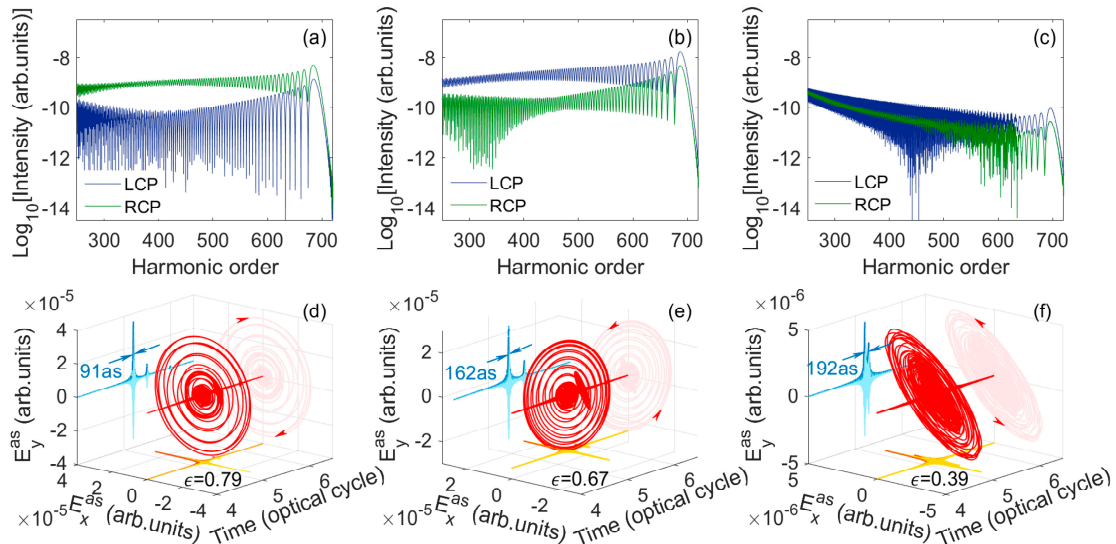


Figure 3. (a–c) The LCP and RCP components of the harmonic spectra generated from the CO molecule oriented at $\theta = 280^\circ$ in the PG laser fields for CEPs, φ_{CE} , of -0.3π , 0.7π , and 0.9π , respectively. (d–f) The 3D plots of the electric fields of the attosecond pulses generated by superposing the harmonics from the 360th to 440th orders, 320th to 360th orders, and 640th to 700th orders in (a–c), respectively. In our simulations, except for the CEP, φ_{CE} , other parameters are the same as those in Figure 1.

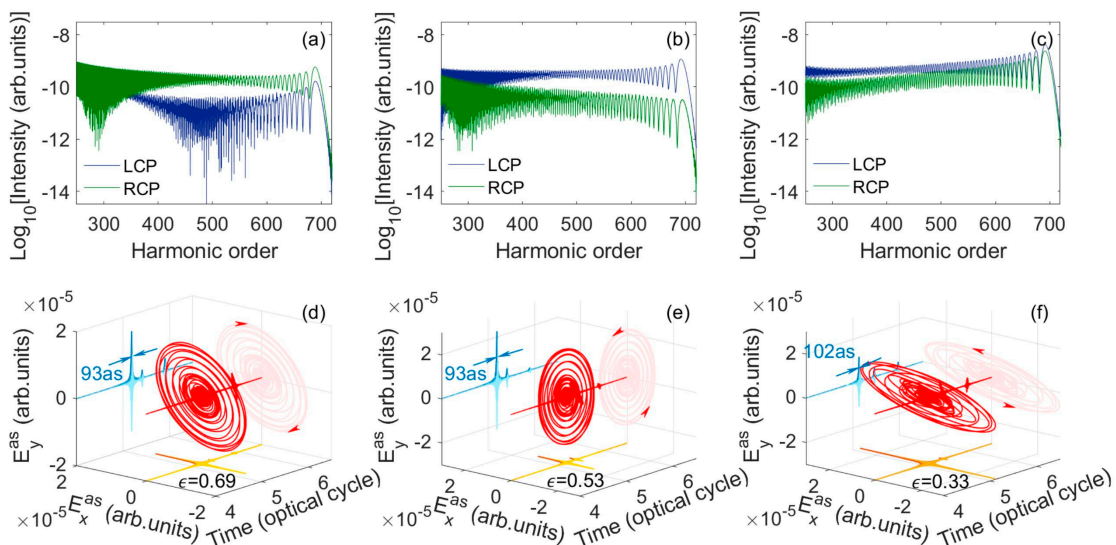


Figure 4. (a–c) The LCP and RCP components of the harmonic spectra generated in the PG laser field for orientation angles, θ , of the CO molecules of 100° , 275° , and 285° , respectively. (d–f) The 3D plots of the electric fields of the attosecond pulses generated by superposing the harmonics from the 460th to 540th orders, 480th to 560th orders, and 310th to 390th orders in (a–c), respectively. In our simulations, except for the orientation angle, θ , other parameters are the same as those in Figure 1.

We extend our scheme to the case of imperfect orientation, considering imperfect molecular orientation in experimental. Figure 5a–f present the harmonic spectra and attosecond pulses in the PG laser field with the CO molecule oriented at $\theta = 280^\circ$ for orientation degrees of 0.8 (a,d), 0.6 (b,e), and 0.4 (d,f), respectively. It is obvious that the orientation degree has an influence on the LCP and RCP harmonic spectra, as well as the generated attosecond pulse. Compared to the case of perfect molecular orientation in Figure 1c,f, the differences between the intensities of the LCP and RCP harmonic components become small in the imperfect orientation situation (see Figure 5a–c), which therefore affect the generated attosecond pulse (see Figure 5d–f). However, by superposing harmonics in the supercontinuum, we can still derive an EP IAP with ellipticity above 0.5 (0.68, 0.71, and 0.5 for orientation degrees of 0.8, 0.6, and 0.4, respectively). It is worth mentioning that several methods have recently been proposed to achieve a high degree of molecular orientation [43–45]. These methods can be combined with our scheme to achieve the generation of largely EP, but even CP IAPs.

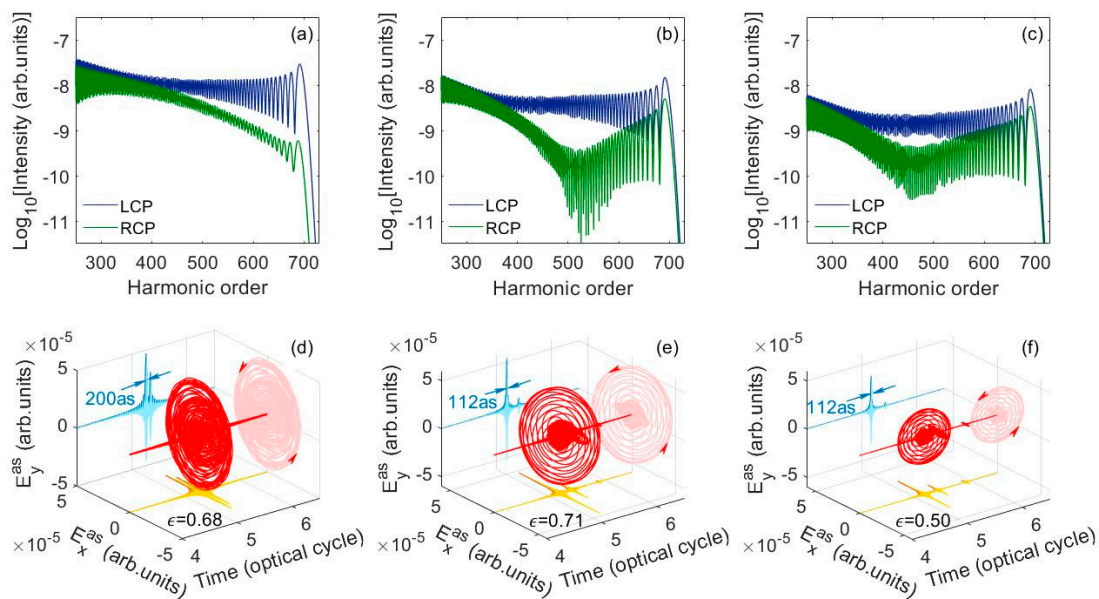


Figure 5. (a–c) The LCP and RCP components of the harmonic spectra generated in the PG laser field with the CO molecule oriented at $\theta = 280^\circ$ for orientation degrees of 0.8, 0.6, and 0.4, respectively. (d–f) The 3D plots of the electric fields of the attosecond pulses generated by superposing the 660th- to 690th-order harmonics, the 490th- to 550th-order harmonics, and the 430th- to 490th-order harmonics in (a–c), respectively.

Finally, we show the universality of our scheme. Figure 6a–d present the harmonic spectra and attosecond pulses generated from the CO molecule oriented at $\theta = 280^\circ$ in the PG laser field with the shorter wavelength and lower intensity than that used in Figure 1. As shown in Figure 6a, in the laser field with an intensity of $3 \times 10^{14} \text{ W/cm}^2$ and wavelength of 1300 nm, the intensity of the LCP harmonic component is higher than that of the RCP component. Therefore, the generated harmonics are with left helicity. By superposing the 280th- to 340th-order harmonics, a left-rotated IAP with an ellipticity of 0.9 and duration of 145 as is obtained, as shown in Figure 6b. As for the case of the PG laser field with an intensity of $2 \times 10^{14} \text{ W/cm}^2$ and wavelength of 1600 nm, the generated high-order harmonics also possess left helicity (see Figure 6c). We can still derive a left-rotated IAP by superposing the 340th- to 400th-order harmonics, as presented in Figure 6d. The ellipticity of this IAP is 0.94, and its duration is 119 as. It is obvious that in these two cases, the generation of LCP harmonics and IAPs from the CO molecule oriented at $\theta = 280^\circ$ is consistent with the result in Figure 1c,f. This indicates that our scheme is feasible with different wavelengths and intensities of the PG laser field.

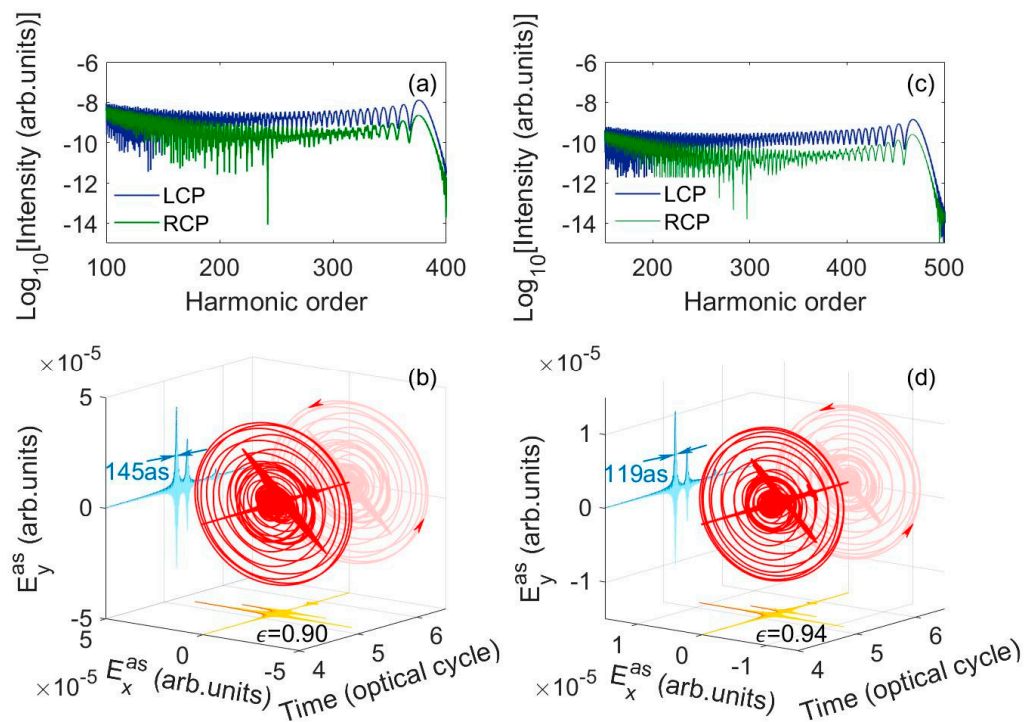


Figure 6. (a) The LCP and RCP components of the harmonic spectra generated from the CO molecule oriented at $\theta = 280^\circ$ in the PG laser field for an intensity of 3×10^{14} W/cm² and a wavelength of 1300 nm. (b) The 3D plots of the electric fields of the attosecond pulses generated by superposing the harmonics from the 280th to 340th orders in (a). (c) Same as (a), but for an intensity of 2×10^{14} W/cm² and a wavelength of 1600 nm. (d) The 3D plots of the electric fields of the attosecond pulses generated by superposing the harmonics from the 340th to 400th orders in (c). In our simulations, except for the wavelength and intensity, other parameters are the same as those in Figure 1 of our manuscript.

4. Conclusions

In conclusion, we have theoretically demonstrated the generation of a CP attosecond pulse with tunable helicity from the interaction of the CO molecule and the PG laser field. Using the time-varying polarization laser field, a broadband supercontinuum with circular polarization is generated from the oriented CO molecule. This supercontinuum enables the production of an IAP with an ellipticity of 0.98 and a duration of 90 as. The generation of a largely EP IAP is robust against the variation in the time delay of the laser field, which can relax the requirements in the experiment. Moreover, we show that through adjusting the CEP of the laser field and the orientation angle of the CO molecule, the helicity of the generated IAP can be effectively controlled. In addition, this scheme can be extended to the PG laser field with different wavelength and intensity. Our work expands the applications of the PG laser field for generating CP high-order harmonics and IAPs with a desired helicity. This capability is beneficial for using these pulse sources in the investigation of chiral-specific dynamics and magnetic circular dichroism on the attosecond timescale.

Author Contributions: Conceptualization, H.Y.; methodology, S.C.; software, S.C.; validation, S.C., H.Y., F.W., and Y.S.; formal analysis, S.C., H.Y., F.W., and Y.S.; investigation, S.C., H.Y., and F.W.; resources, H.Y., F.W., and Y.S.; data curation, S.C., H.Y., F.W., and Y.S.; writing—original draft preparation, H.Y. and S.C.; writing—review and editing, S.C., H.Y., F.W., J.S., Y.Z., C.Y., T.O., R.Z., Q.C., and Y.S.; visualization, S.C., H.Y., F.W., J.S., Y.Z., C.Y., T.O., R.Z., Q.C., and Y.S.; supervision, H.Y., F.W., and Y.S.; project administration, H.Y., F.W., and Y.S.; funding acquisition, H.Y., F.W., and Y.S. All authors have read and agreed to the published version of the manuscript.

Funding: This research was funded by the National Natural Science Foundation of China (NSFC), grant numbers 12204279, 12104349, and 11974108, and the Campus Science Foundation Research Project of Wuhan Institute of Technology, China, grant number K2021076.

Institutional Review Board Statement: Not applicable.

Informed Consent Statement: Not applicable.

Data Availability Statement: The data supporting the findings of this study are available from the corresponding author upon reasonable request.

Conflicts of Interest: The authors declare no conflicts of interest.

References

1. Corkum, P.B.; Krausz, F. Attosecond science. *Nat. Phys.* **2007**, *3*, 381–387. [[CrossRef](#)]
2. Chatziathanasiou, S.; Kahaly, S.; Skantzakis, E.; Sansone, G.; Lopez-Martens, R.; Haessler, S.; Varju, K.; Tsakiris, G.; Charalambidis, D.; Tzallas, P. Generation of Attosecond Light Pulses from Gas and Solid State Media. *Photonics* **2017**, *4*, 26. [[CrossRef](#)]
3. Corkum, P.B. Plasma perspective on strong field multiphoton ionization. *Phys. Rev. Lett.* **1993**, *71*, 1994–1997. [[CrossRef](#)] [[PubMed](#)]
4. Bartels, R.A.; Paul, A.; Green, H.; Kapteyn, H.C.; Murnane, M.M.; Backus, S.; Christov, I.P.; Liu, Y.; Attwood, D.; Jacobsen, C. Generation of Spatially Coherent Light at Extreme Ultraviolet Wavelengths. *Science* **2002**, *297*, 376–378. [[CrossRef](#)] [[PubMed](#)]
5. Popmintchev, T.; Chen, M.-C.; Arpin, P.; Murnane, M.M.; Kapteyn, H.C. The attosecond nonlinear optics of bright coherent X-ray generation. *Nat. Photonics* **2010**, *4*, 822–832. [[CrossRef](#)]
6. Itatani, J.; Quéré, F.; Yudin, G.L.; Ivanov, M.Y.; Krausz, F.; Corkum, P.B. Attosecond Streak Camera. *Phys. Rev. Lett.* **2002**, *88*, 173903. [[CrossRef](#)] [[PubMed](#)]
7. Greening, D.; Weaver, B.; Pettipher, A.J.; Walke, D.J.; Larsen, E.W.; Marangos, J.P.; Tisch, J.W.G. Generation and measurement of isolated attosecond pulses with enhanced flux using a two colour synthesized laser field. *Opt. Express* **2020**, *28*, 23329. [[CrossRef](#)] [[PubMed](#)]
8. Kienberger, R.; Goulielmakis, E.; Uiberacker, M.; Baltuska, A.; Yakovlev, V.; Bammer, F.; Scrinzi, A.; Westerwalbesloh, T.; Kleineberg, U.; Heinzmann, U.; et al. Atomic transient recorder. *Nature* **2004**, *427*, 817–821. [[CrossRef](#)]
9. Goulielmakis, E.; Schultze, M.; Hofstetter, M.; Yakovlev, V.S.; Gagnon, J.; Uiberacker, M.; Aquila, A.L.; Gullikson, E.M.; Attwood, D.T.; Kienberger, R.; et al. Single-Cycle Nonlinear Optics. *Science* **2008**, *320*, 1614–1617. [[CrossRef](#)]
10. Pfeifer, T.; Gallmann, L.; Abel, M.J.; Nagel, P.M.; Neumark, D.M.; Leone, S.R. Heterodyne mixing of laser fields for temporal gating of high-order harmonic generation. *Phys. Rev. Lett.* **2006**, *97*, 163901. [[CrossRef](#)]
11. Lan, P.; Takahashi, E.J.; Midorikawa, K. Optimization of infrared two-color multicycle field synthesis for intense-isolated-attosecond-pulse generation. *Phys. Rev. A* **2010**, *82*, 053413. [[CrossRef](#)]
12. Haessler, S.; Balčiūnas, T.; Fan, G.; Chipperfield, L.E.; Baltuška, A. Enhanced multi-colour gating for the generation of high-power isolated attosecond pulses. *Sci. Rep.* **2015**, *5*, 10084. [[CrossRef](#)] [[PubMed](#)]
13. Yuan, H.; He, L.; Wang, F.; Wang, B.; Liu, W.; Hong, Z. Generation of isolated attosecond pulses in a multi-cycle inhomogeneous two-color field without CEP stabilization. *Opt. Quantum Electron.* **2017**, *49*, 214. [[CrossRef](#)]
14. Xue, B.; Tamaru, Y.; Fu, Y.; Yuan, H.; Lan, P.; Mücke, O.D.; Suda, A.; Midorikawa, K.; Takahashi, E.J. Fully stabilized multi-TW optical waveform synthesizer: Toward gigawatt isolated attosecond pulses. *Sci. Adv.* **2020**, *6*, eaay2802. [[CrossRef](#)] [[PubMed](#)]
15. Chang, Z. Chirp of the single attosecond pulse generated by a polarization gating. *Phys. Rev. A* **2005**, *71*, 023813. [[CrossRef](#)]
16. Sansone, G.; Benedetti, E.; Calegari, F.; Vozzi, C.; Avaldi, L.; Flammini, R.; Poletto, L.; Villoresi, P.; Altucci, C.; Velotta, R.; et al. Isolated single-cycle attosecond pulses. *Science* **2006**, *314*, 443–446. [[CrossRef](#)]
17. Sola, I.J.; Mével, E.; Elouga, L.; Constant, E.; Strelkov, V.; Poletto, L.; Villoresi, P.; Benedetti, E.; Caumes, J.P.; Stagira, S.; et al. Controlling attosecond electron dynamics by phase-stabilized polarization gating. *Nat. Phys.* **2006**, *2*, 319–322. [[CrossRef](#)]
18. Zhang, Q.; Lu, P.; Lan, P.; Hong, W.; Yang, Z. Multi-cycle laser-driven broadband supercontinuum with a modulated polarization gating. *Opt. Express* **2008**, *16*, 9795–9803. [[CrossRef](#)] [[PubMed](#)]
19. Gaumnitz, T.; Jain, A.; Pertot, Y.; Huppert, M.; Jordan, I.; Ardana-Lamas, F.; Wörner, H.J. Streaking of 43-attosecond soft-X-ray pulses generated by a passively CEP-stable mid-infrared driver. *Opt. Express* **2017**, *25*, 27506. [[CrossRef](#)]
20. Li, J.; Ren, X.; Yin, Y.; Zhao, K.; Chew, A.; Cheng, Y.; Cunningham, E.; Wang, Y.; Hu, S.; Wu, Y.; et al. 53-attosecond X-ray pulses reach the carbon K-edge. *Nat. Commun.* **2017**, *8*, 186. [[CrossRef](#)]
21. Böwering, N.; Lischke, T.; Schmidtke, B.; Müller, N.; Khalil, T.; Heinzmann, U. Asymmetry in Photoelectron Emission from Chiral Molecules Induced by Circularly Polarized Light. *Phys. Rev. Lett.* **2001**, *86*, 1187–1190. [[CrossRef](#)] [[PubMed](#)]
22. López-Flores, V.; Arabski, J.; Stamm, C.; Halté, V.; Pontius, N.; Beaurepaire, E.; Boeglin, C. Time-resolved x-ray magnetic circular dichroism study of ultrafast demagnetization in a CoPd ferromagnetic film excited by circularly polarized laser pulse. *Phys. Rev. B* **2012**, *86*, 014424. [[CrossRef](#)]
23. Siegrist, F.; Gessner, J.A.; Osslander, M.; Denker, C.; Chang, Y.-P.; Schröder, M.C.; Guggenmos, A.; Cui, Y.; Walowski, J.; Martens, U.; et al. Light-wave dynamic control of magnetism. *Nature* **2019**, *571*, 240–244. [[CrossRef](#)] [[PubMed](#)]
24. Baykusheva, D.; Wörner, H.J. Chiral Discrimination through Bielliptical High-Harmonic Spectroscopy. *Phys. Rev. X* **2018**, *8*, 031060. [[CrossRef](#)]

25. Ferré, A.; Handschin, C.; Dumergue, M.; Burgy, F.; Comby, A.; Descamps, D.; Fabre, B.; Garcia, G.A.; Géneaux, R.; Merceron, L.; et al. A table-top ultrashort light source in the extreme ultraviolet for circular dichroism experiments. *Nat. Photonics* **2014**, *9*, 93–98. [[CrossRef](#)]
26. Vodungbo, B.; Barszczak Sardinha, A.; Gautier, J.; Lambert, G.; Valentin, C.; Lozano, M.; Iaquaniello, G.; Delmotte, F.; Sebban, S.; Lüning, J.; et al. Polarization control of high order harmonics in the EUV photon energy range. *Opt. Express* **2011**, *19*, 4346–4356. [[CrossRef](#)]
27. Zhang, J.; Wang, S.; Huo, X.-X.; Xing, Y.-H.; Wang, F.; Liu, X.-S. Generation of ellipticity-tunable isolated attosecond pulses from diatomic molecules in intense laser fields. *Opt. Commun.* **2023**, *530*, 129152. [[CrossRef](#)]
28. Sun, F.J.; Chen, C.; Li, W.Y.; Liu, X.; Li, W.; Chen, Y.J. High ellipticity of harmonics from molecules in strong laser fields of small ellipticity. *Phys. Rev. A* **2021**, *103*, 053108. [[CrossRef](#)]
29. Fleischer, A.; Kfir, O.; Diskin, T.; Sidorenko, P.; Cohen, O. Spin angular momentum and tunable polarization in high-harmonic generation. *Nat. Photonics* **2014**, *8*, 543–549. [[CrossRef](#)]
30. Kfir, O.; Grychtol, P.; Turgut, E.; Knut, R.; Zusin, D.; Popmintchev, D.; Popmintchev, T.; Nembach, H.; Shaw, J.M.; Fleischer, A.; et al. Generation of bright phase-matched circularly-polarized extreme ultraviolet high harmonics. *Nat. Photonics* **2014**, *9*, 99–105. [[CrossRef](#)]
31. Fan, T.; Grychtol, P.; Knut, R.; Hernández-García, C.; Hickstein, D.D.; Zusin, D.; Gentry, C.; Dollar, F.J.; Mancuso, C.A.; Hogle, C.W.; et al. Bright circularly polarized soft X-ray high harmonics for X-ray magnetic circular dichroism. *Proc. Natl. Acad. Sci. USA* **2015**, *112*, 14206–14211. [[CrossRef](#)] [[PubMed](#)]
32. Dorney, K.M.; Ellis, J.L.; Hernández-García, C.; Hickstein, D.D.; Mancuso, C.A.; Brooks, N.; Fan, T.; Fan, G.; Zusin, D.; Gentry, C.; et al. Helicity-Selective Enhancement and Polarization Control of Attosecond High Harmonic Waveforms Driven by Bichromatic Circularly Polarized Laser Fields. *Phys. Rev. Lett.* **2017**, *119*, 063201. [[CrossRef](#)] [[PubMed](#)]
33. Jiménez-Galán, Á.; Zhavoronkov, N.; Ayuso, D.; Morales, F.; Patchkovskii, S.; Schloz, M.; Pisanty, E.; Smirnova, O.; Ivanov, M. Control of attosecond light polarization in two-color bicircular fields. *Phys. Rev. A* **2018**, *97*, 023409. [[CrossRef](#)]
34. Huang, P.-C.; Hernández-García, C.; Huang, J.-T.; Huang, P.-Y.; Lu, C.-H.; Rego, L.; Hickstein, D.D.; Ellis, J.L.; Jaron-Becker, A.; Becker, A.; et al. Polarization control of isolated high-harmonic pulses. *Nat. Photonics* **2018**, *12*, 349–354. [[CrossRef](#)]
35. Fang, Y.; Liu, Y. Optimal control over high-order-harmonic ellipticity in two-color cross-linearly-polarized laser fields. *Phys. Rev. A* **2021**, *103*, 033116. [[CrossRef](#)]
36. Zhou, X.; Lock, R.; Wagner, N.; Li, W.; Kapteyn, H.C.; Murnane, M.M. Elliptically Polarized High-Order Harmonic Emission from Molecules in Linearly Polarized Laser Fields. *Phys. Rev. Lett.* **2009**, *102*, 073902. [[CrossRef](#)]
37. Le, A.-T.; Lucchese, R.R.; Lin, C.D. Polarization and ellipticity of high-order harmonics from aligned molecules generated by linearly polarized intense laser pulses. *Phys. Rev. A* **2010**, *82*, 023814. [[CrossRef](#)]
38. Zhai, C.; Wu, Y.; Liu, Y.; Zhang, K.; Kang, S.; Li, Z.; Wu, F.; Dong, X.; Cheng, X.; Li, Y.; et al. Near-circularly polarized isolated attosecond pulse generation from gas mixture with two-color multicycle laser fields. *Results Phys.* **2024**, *58*, 107518. [[CrossRef](#)]
39. Van der Zwan, E.V.; Lein, M. Two-center interference and ellipticity in high-order harmonic generation from H_2^+ . *Phys. Rev. A* **2010**, *82*, 033405. [[CrossRef](#)]
40. Strelkov, V.V.; Gonoskov, A.A.; Gonoskov, I.A.; Ryabikin, M.Y. Origin for ellipticity of high-order harmonics generated in atomic gases and the sublaser-cycle evolution of harmonic polarization. *Phys. Rev. Lett.* **2011**, *107*, 043902. [[CrossRef](#)]
41. Lewenstein, M.; Balcou, P.; Ivanov, M.Y.; L’huillier, A.; Corkum, P.B. Theory of high-harmonic generation by low-frequency laser fields. *Phys. Rev. A* **1994**, *49*, 2117. [[CrossRef](#)]
42. Tong, X.M.; Zhao, Z.X.; Lin, C.-D. Theory of molecular tunneling ionization. *Phys. Rev. A* **2002**, *66*, 033402. [[CrossRef](#)]
43. Huang, Y.; Xie, T.; Li, J.; Yu, J.; Cong, S.-L. Efficiently field-free orientation of CO molecules by a femtosecond pulse and a THz pulse train. *Laser Phys.* **2014**, *24*, 016002. [[CrossRef](#)]
44. Dang, H.-P.; Wang, S.; Zhan, W.; Han, X.-F.; Zai, J.-B. Field-free molecular orientation by two-color femtosecond laser pulse and time-delayed THz laser pulse. *Laser Phys.* **2015**, *25*, 075301. [[CrossRef](#)]
45. Liao, S.-L.; Ho, T.-S.; Rabitz, H.; Chu, S.-I. Maximum attainable field-free molecular orientation of a thermal ensemble with near—single-cycle THz pulses. *Phys. Rev. A* **2013**, *87*, 013429. [[CrossRef](#)]

Disclaimer/Publisher’s Note: The statements, opinions and data contained in all publications are solely those of the individual author(s) and contributor(s) and not of MDPI and/or the editor(s). MDPI and/or the editor(s) disclaim responsibility for any injury to people or property resulting from any ideas, methods, instructions or products referred to in the content.